

The challenge of developing rechargeable magnesium batteries

Ivgeni Shterenberg, Michael Salama, Yossi Gofer, Elena Levi, and Doron Aurbach

The high specific capacity, reactivity, and abundance of magnesium in the earth's crust and the relatively good safety features of Mg metal, despite its being a reactive metal, drive intensive efforts to develop rechargeable Mg batteries as a follow-up to the success of Li-ion battery technology. However, Mg anodes cannot function in usual non-aqueous electrolyte solutions. Consequently, it is important to develop unique, complex solutions for reversible Mg metal anodes. Also, finding relevant cathode materials that can reversibly insert bivalent Mg ions is a great challenge. In this article, we review the efforts and success in the development of several families of electrolyte solutions for secondary Mg batteries, in which Mg anodes behave fully reversibly, but also exhibit the necessary wide electrochemical window. We also review attempts to develop positive electrodes for rechargeable Mg batteries. The first generation of secondary Mg batteries has already been demonstrated, but their specific energy density remains relatively low. The challenge now is to develop novel Mg battery prototypes that possess high energy density.

Introduction

Mobile devices play an increasingly important role in our everyday lives, from laptop computers and cellular phones to electric vehicles. A major impediment to further develop such devices is the quality of their power sources. These devices should possess high energy densities, operate over a wider temperature range, be user-friendly (low toxicity of components), exhibit prolonged cycle life, and, most importantly, have low manufacturing and handling costs. Lithium-ion batteries can be considered the current leading technology for energy storage and conversion. However, disadvantages of Li-based battery technology are high cost and safety concerns. Mg batteries may provide a safe and cheap alternative to Li-ion battery technology in various applications.

Magnesium metal is an ideal anode material[1] for rechargeable batteries. It possesses a low reduction potential of –2.37 V (H^+/H_2 scale, the lowest reduction potential after Li, –3 V), a high volumetric capacity of 3,833 mA h cm^{-3} (2,046 mA h cm^{-3} for Li), lower price, and high abundance (eighth most abundant element in the earth's crust). However, there are many challenges with implementing Mg as a viable anode for rechargeable batteries, with the most challenging being overcoming the formation of passivating layers. Magnesium is a highly reactive metal, and passivation layers are rapidly formed on the Mg surface when in contact with reducible species such as water, oxygen, and various organics. Unlike the layers formed on Li metal that conduct Li ions, the layers formed on Mg are truly passivating and completely block conduction of Mg ions. The formation of passivating layers on Mg limits the selection of a suitable electrolyte solution; the solvents and salts must be stable with Mg and create a passivation-free environment to allow reversible Mg deposition and stripping.

The first suitable electrolyte for reversible Mg deposition/stripping was reported in the 1920s.[2] The electrolyte was based on Grignard reagents (R-MgX, R = C_6H_5 X = Br,Cl), whose reductive nature made them stable for Mg metal and made it passivation-layer free. Grignard solutions, however, were unsuitable for practical use due to their extremely low conductivity (on the scale of a few μS cm^{-1}) and low anodic stability, which results in a narrow electrochemical window (<1 V) (advanced electrolyte solutions for Li batteries exhibit an electrochemical window of up to 5V). Gregory et al.[3] conducted further research during the 1980s, with the most significant finding being the non-Grignard magnesium organo-borate

Ivgeni Shterenberg, Chemistry Department, Bar-Ilan University, Israel; suttercaine666@gmail.com
Michael Salama, Chemistry Department, Bar-Ilan University, Israel; 123salama@gmail.com
Yossi Gofer, Chemistry Department, Bar-Ilan University, Israel; goferyosef@gmail.com
Elena Levi, Department of Chemistry, Bar-Ilan University, Israel; elenal@mail.biu.ac.il
Doron Aurbach, Department of Chemistry, Bar-Ilan University, Israel; aurbach@mail.biu.ac.il
DOI: 10.1557/mrs.2014.61

© 2014 Materials Research Society

https://doi.org/10.1557/mrs.2014.61 Published online by Cambridge University Press

electrolyte (0.25 M $Mg(BBu_2Ph_2)_2$ in tetrahydrofuran [THF]; Bu = butyl; Ph = phenyl). Still, such solutions were impractical due to the narrow electrochemical window (<2 V).

An additional major challenge is the integration of cathode materials that allow electrochemical insertion of divalent Mg^{2+} ions. The high charge/radius of Mg^{2+} ions causes a strong interaction with ions in the host material (the cathode), which severely hampers the insertion kinetics of Mg^{2+} ions. Screening of a wide array of cathode materials showed that Mg ions fail to intercalate into most metal oxides and sulfides. The most notable cathode material that could reversibly intercalate Mg^{2+} ions was Mo_6S_8, the so-called Chevrel-phase, first presented in 1971.[4] This article summarizes and presents significant achievements in rechargeable Mg systems over the last decade.

Grignard-based electrolytes for Mg rechargeable batteries

The first Mg battery prototype and dichloro complex solutions

In 2000, Aurbach et al. presented the first prototype system for a Mg battery. The prototype system consisted of a Mg anode, a Mo_6S_8 Chevrel phase cathode, and an electrolyte solution based on an organohaloaluminate salt.[5] **Figure 1**[5] illustrates, by using actual response curves, the electrochemical machinery and shows the operation scheme of the first rechargeable Mg battery system developed, depicting deposition/stripping on the anode side and intercalation/deintercalation on the cathode side. The organohaloaluminate electrolyte solution was composed of the products of the acid-based reaction between the R_mMgCl_{2-m} Lewis base and an R_nAlCl_{3-n} (R = alkyl, aryl) Lewis acid. Following screening of various Lewis base and Lewis acid combinations, the optimal solution in terms of electrochemical behavior was found. The most optimal solution was named the dichloro complex (DCC), and was composed of the product of the reaction between one equivalent of Bu_2Mg with two equivalents of $EtAlCl_2$ (Et = ethyl). The DCC solution showed high ionic conductivity of 1.4 mS cm^{-1}, a 100% Mg deposition/stripping reversibility, and a very wide electrochemical window of up to 2.4 V.

Following further study on organohaloaluminate-based solutions,[6–10] major conclusions were made:

- The reaction between the magnesium and aluminum species results in a full transmetallation (the transfer of ligands from one metal to another) process in which the organic ligands are transferred to the aluminum, while the chloride ligands are transferred to the magnesium. This reaction yields the crucial species for the operation of the magnesium cells in addition to the generation of ions in the solution, thus imparting good ionic conductivity. In the optimum stoichiometries, the Mg-based ions support reversible magnesium deposition and intercalation-liable Mg^{2+} ions.
- The aluminum species were found to maintain a coordination number of four, coordinated by a combination of organic, chloride, or THF ligands. The magnesium species maintained a coordination number of six. Dimers bridged by chlorides were also observed. The main Mg species present in the solution are $MgCl^+$, Mg_2Cl^{3+}, and $MgCl_2$. This arrangement yields solutions possessing wider electrochemical stability windows than those of the Grignard reagents solely.
- Chlorine as an inorganic ligand gives the widest anodic stability (voltage).
- The electrochemical stability window is governed by the Cl:R (organic group) ratios. The higher the chloride to R ligands ratio, the wider is the electrochemical window. This can be explained by the fact that the chlorides reduce the electron density of the aluminum, which in turn polarizes the Al–R bonds, making them more resistant to oxidation. Also, higher chloride to R ligands ratios result in fewer Al–R bonds, which significantly lowers the probability of oxidation.
- The electrochemical window is limited by the β-H elimination reaction, the elimination of hydrogen on the β carbon (i.e., the carbon bonded to the carbon that has a direct chemical bond with the metal atom, Al in our case) occurring on the organic ligand. Indeed, using organic ligands that are resistant to β-H elimination such as methyl, phenyl, or HMDS (hexamethyldisilazane) results in a wider electrochemical window.

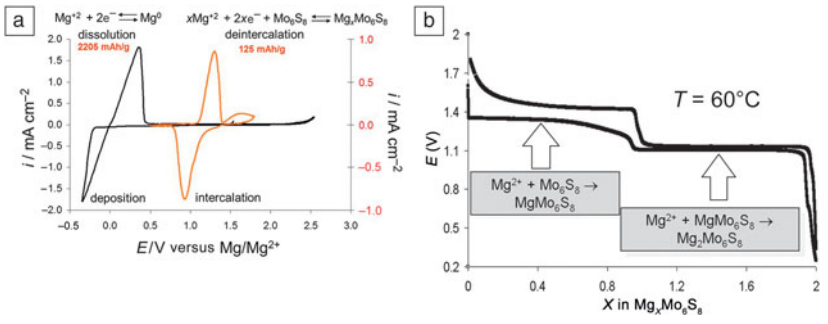


Figure 1. (a) Operation schemes of a Mg rechargeable battery composed of a Chevrel-phase Mo_6S_8 cathode, a Mg metal anode, and an electrolyte solution based on dichloro complex (DCC)/tetrahydrofuran. The relevant electrochemical responses of each half-cell reaction are presented in the black and orange curves. The black curve is acquired during deposition/stripping of Mg, while the orange curve shows the response of a Mo_6S_8 cathode during intercalation/deintercalation of Mg ions. From these response curves, one can assess the open circuit voltage of a full cell as well as the working potentials. (b) Typical galvanostatic charge-discharge curves for a complete cell containing a Mo_6S_8 cathode and a Mg anode in a DCC solution. At 60°C, no trapping effect occurs, leading to 100% faradaic reversibility and small hysteresis voltage differences. Each of the two plateaus observed, both in the charging and the discharging curves, pertains to the phase transitions denoted in the schemes.[5] Note: *T*, temperature; *i*, current; *E*, voltage.

Advanced Grignard-based solutions with high anodic stability

Rigorous study[6–10] on organohaloaluminate-based solutions concluded that the oxidation stability window is limited by β-H elimination,

https://doi.org/10.1557/mrs.2014.61 Published online by Cambridge University Press

as mentioned previously. Therefore, substituting the organic ligand group for ligands that contain no hydrogen atoms on the β position would render β-H elimination implausible and thus extend the electrochemical window. Two notable electrolyte solutions are presented in this section.

The Aurbach group developed the first solution, the all phenyl complex (APC) electrolyte solution.[11] The APC solution is composed of the reaction products between Ph_xMgCl_{2-x} and Ph_yAlCl_{3-y}. Indeed, the anodic stability window in the APC solutions is high and reaches 3.3 V. These solutions also show high Coulombic efficiency up to 100%, a low over-potential for deposition (below 2 V), and a specific conductivity of 2 mS/cm at room temperature.

Figure 2b shows a typical cyclic voltammogram of standard APC solutions. Pour et al.[11] conducted a rigorous study on the identification of the equilibrium species in APC solutions. The identification was carried out by Raman spectroscopy, multinuclear nuclear magnetic resonance, and single-crystal x-ray diffraction (XRD) analyses, in conjunction with density functional theory quantum mechanical calculations. The equilibrium species present in the standard APC solution are Ph_4Al^-, $Ph_2AlCl_2^-$, $PhAlCl_3^-$, $AlCl_4^-$, and $Mg_2Cl_3^+$. Based on this research, the following reaction formula is suggested for the formation of the standard APC solution:

$$9PhMgCl + 4.5AlCl_3 \rightarrow Ph_4Al^- + 2Ph_2AlCl_2^- + PhAlCl_3^- + 0.5AlCl_4^- + 4.5Mg_2Cl_3^+. \quad (1)$$

The second notable electrolyte solution contains HMDS as the organic ligand. Libenow et al. reported in 2000 that HMDSMgCl can be reversibly stripped/deposited from solutions containing ether solvents.[12] Kim et al.[13] conducted a significant investigation of HMDSMgCl electrolyte solution. The low nucleophilic nature of HMDSMgCl makes it compatible with sulfur cathodes. The energy density for a battery composed of a sulfur cathode coupled with a Mg anode is estimated to be 4000 Wh/L, which is twice that of a Li battery. Kim et al. have shown[13] that the addition of $AlCl_3$ to HMDSMgCl increases the current density by an order of seven. They were also able to successfully re-crystallize the active species in an HMDSMgCl/$AlCl_3$ (THF) solution and thus widen the electrochemical window by 0.8 V and achieve a Coulombic efficiency of 100%. Figure 2a shows a comparison between HMDSMgCl (THF), HMDSMgCl/$AlCl_3$ (THF), and re-crystallized HMDSMgCl/$AlCl_3$ (THF) solutions. A fully assembled cell containing sulfur as the cathode and Mg as the anode with a re-crystallized HMDSMgCl/$AlCl_3$ (THF) solution displayed an excellent capacity of 1200 mAh/g for the first discharge. However, the second discharge showed significant capacity fading. It is theorized that the capacity fading is due to polysulphide or sulfur dissolution.

Non-Grignard based solutions

Magnesium aluminum chloro complex

Implementing Grignard reagents in actual batteries would be impractical due to the reagent's high cost, high hazard level, and high susceptibility toward oxidation. Developing non-organo-metallic-based solutions for Mg batteries is crucial for real-life battery systems. The magnesium aluminum chloro complex (MACC) solutions developed at Bar-Ilan University and Pellion Technologies consist fully of inorganic salts.[14]

The MACC solutions are composed of the reaction products between $MgCl_2$ and $AlCl_3$ in THF or glyme (poly-ether) solvents. The MACC solutions are endowed with high Mg deposition/stripping cycling efficiency of up to <99%, low over-potential for magnesium deposition, and a high electrochemical window of 3.1 V (**Figure 3**a).[14] Reversible intercalation/deintercalation of Mg ions into Chevrel-phase Mo_6S_8 from a MACC solution was also demonstrated. It is believed that combining $MgCl_2$ and $AlCl_3$ results in an acid–base reaction, much like the transmetallation reaction with Grignard-based electrolytes. This assumption is supported by two observations: (1) $MgCl_2$ by itself has low solubility in THF, and the addition of $AlCl_3$ significantly increases solubility and forms clear solutions with high Mg ion concentrations, which is important for rapid magnesium deposition/dissolution processes, as well as for Mg intercalation into host materials. (2) Significant increases in conductivity, up to the mS range, are observed when mixing $MgCl_2$ and $AlCl_3$, indicating the formation of ionic species. The $MgCl_2$–$AlCl_3$ reaction most probably involves, based on previous studies with Grignard-based electrolytes, chloride migration between Mg and Al to form various active magnesium ionic species such as $MgCl^+$ and $Mg_2Cl_3^+$.

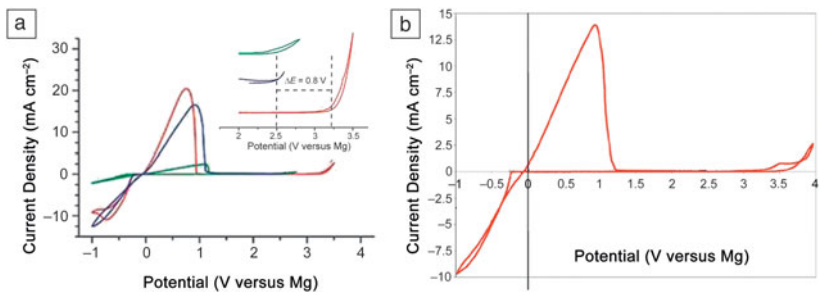


Figure 2. (a) Cyclic voltammograms of HMDSMgCl (green, HMDS = hexamethyldisilazane), HMDSMgCl with $AlCl_3$ (blue), and re-crystallized HMDSMgCl + $AlCl_3$ (red) solutions. The inset is an enlargement of the electrochemical window limit. The voltammogram shows how re-crystallization of the electrolyte solution significantly widens the electrochemical window by 0.8 V.[13] (b) Typical cyclic voltammogram of solutions comprising THF (tetrahydrofuran), PhMgCl (Ph = phenyl), and $AlCl_3$. These systems are denoted as all phenyl complex (APC) solutions. The active species in solutions are $MgCl^+$ and $Mg_2Cl_3^+$ cations stabilized by THF molecules and $AlCl_{4-n}Ph_n^-$ anions (formed by transmetallation reactions in solution).[11] The APC solution is highly reversible and shows a significant increase in the electrochemical window compared to the previous Grignard-based solutions (DCC). Note: Δ*E*, extension (in volts) of the electrochemical window following re-crystallization.

https://doi.org/10.1557/mrs.2014.61 Published online by Cambridge University Press

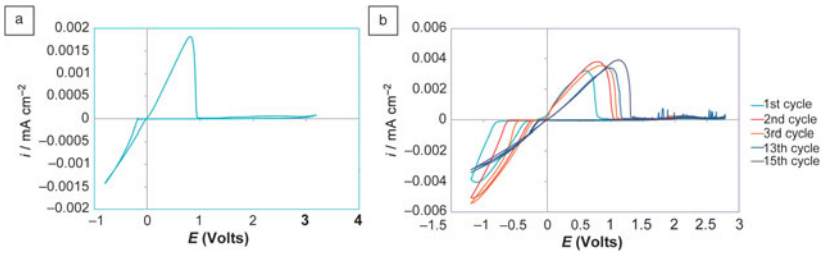


Figure 3. Inorganic salt-based electrolyte solutions. (a) Cyclic voltammogram of conditioned $MgCl_2$-$AlCl_3$/THF (MACC; THF = tetrahydrofuran) solution. The MACC solution exhibits electrochemical performance on par with all phenyl complex solutions, with the added benefit of not containing the highly hazardous Grignard reagents. (b) Selected cycles during the conditioning procedure. Although not yet understood, the conditioning procedure highly enhances the electrochemical performance of MACC solutions, especially the reversibility and overpotential for deposition.[14]

Normally, solutions consisting of $MgCl_2$ and $AlCl_3$ show very poor magnesium deposition/dissolution reversibility. However, it was discovered through serendipity that by electrochemical "conditioning," it is possible to significantly enhance the electrochemical characteristics of such solutions. The electrochemical conditioning consists of cycling the solutions in a sealed cell, using Pt as the working electrode and Mg foil as the counter electrode, between the potentials of –1.2 V and 2.8 V at a scan rate of 1 mV/sec. The number of cycles that is required in order to achieve maximum electrochemical properties enhancement depends on the amount of solution used, approximately 15 cycles for 10 mL solution. Figure 3b[14] shows selected cycles of the conditioning process on $MgCl_2$ (0.25M)+$AlCl_3$(0.075M) 20 mL solution. The first cycle is consistent with the standard behavior of $MgCl_2$/$AlCl_3$ solutions, as it displays very poor reversibility, large over-potential for magnesium deposition, and wide hysteresis. Each consecutive cycle, though, shows significant improvement in electrochemical characteristics: the overpotential for magnesium deposition decreases, the cycling efficiency increases, and the hysteresis narrows. Once the MACC solution has been conditioned, it retains its enhanced electrochemical characteristics even after three months in storage.

As of yet, the conditioning process is not fully understood. It is hypothesized that during the process, water residue is eliminated. Removal of water residue prevents the formation of passivating layers that are non-conductive to bivalent magnesium ions. In Grignard-based electrolytes, water residue is usually not a hindrance since Grignard reagents act as water scavengers. This research has shown that non-Grignard non-organometallic-based electrolyte solutions with excellent electrochemical characteristics can be implemented in Mg secondary batteries. This study is an important step forward, away from Grignard/organo-metallic based-electrolytes and toward more "simple salt"-based systems.

$MgTFSI_2$-based electrolytes

One of the "holy grails" of magnesium battery research is to implement electrolyte solutions based on simple salts such as $Mg(TFSI)_2$ (TFSI = trifluoromethanesulfonimide). Such a simple salt is easily dissolved in various organic solvents and ionic liquids (ILs), shows high conductivity, does not contain corrosive elements (such as chlorides), and therefore is stable with most cathode materials. Additionally, $Mg(TFSI)_2$ is highly resistive to oxidation and allows a wide voltage operation. However, compatibility of $Mg(TFSI)_2$ with Mg anodes is still in question, and reversible Mg deposition/stripping from $Mg(TFSI)_2$ salt has been proven to be difficult.

Research by Shimamura et al. has shown some success in reversibly depositing/stripping Mg as an alloy or composite from a $Mg(TFSI)_2$/LiTFSI in an IL solution.[15] ILs (see the July 2013 issue of *MRS Bulletin*) are good candidates to replace ethers in practical Mg batteries due to their non-volatile non-flammable nature, high conductivity, and high electrochemical window of up to 6V. Due to the difficulty of depositing pure Mg metal from a $Mg(TFSI)_2$ (in IL) solution, it was suggested that deposition of a binary alloy or composite containing Mg and Li might be possible. **Figure 4**a[15] shows cyclic voltammograms for different compositions of IL-based electrolytes. As expected, the $Mg(TFSI)_2$ solution exhibited no reversible Mg deposition/stripping, while the LiTFSI solution exhibited typical reversible behavior for Li deposition/stripping. Interestingly, the solution containing both $Mg(TFSI)_2$ and LiTFSI exhibited

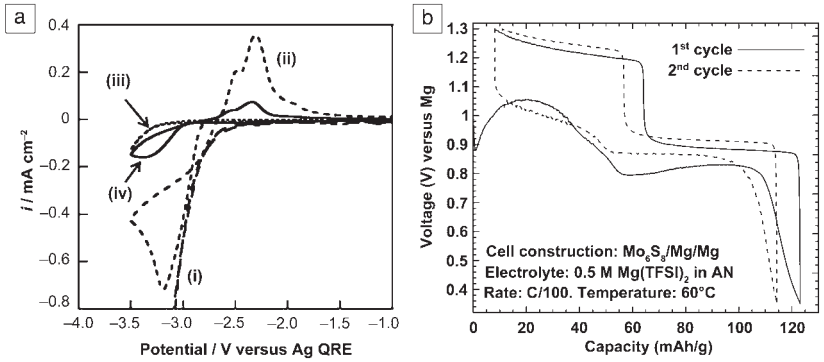


Figure 4. (a) Cyclic voltammograms of (i) *N*,*N*-diethyl-*N*-methyl-*N*-(2-methoxyethyl) ammonium bis(trifluoromethylsulfonyl)imide (DEME-TFSI), (ii) DEME-TFSI dissolving 20 mol% LiTFSI, (iii) DEME-TFSI dissolving 20 mol% $Mg(TFSI)_2$, and (iv) DEME-TFSI dissolving mixed 10 mol% LiTFSI and 10 mol% $Mg(TFSI)_2$. The voltammograms show that although Mg cannot be deposited from a $Mg(TFSI)_2$ solution (curve iii), co-deposition of Li and Mg is possible when adding LiTFSI (curve iv).[15] (b) Voltage profile of a Mo_6S_8/Mg/Mg three electrode cell with 0.5 M $Mg(TFSI)_2$ in acetonitrile (AN) solution operating at 60°C. The voltage profile shows that it is possible, in fact, to intercalate Mg ions into a Mo_6S_8 cathode from a $Mg(TFSI)_2$-based solution with relatively good capacitance.[16] Note: *i*, current; *E*, voltage; QRE, quasi reference electrode; C, charge rate.

https://doi.org/10.1557/mrs.2014.61 Published online by Cambridge University Press

reversible deposition/stripping of a Li/Mg composite. The presence of a hexagonal Mg plane, with no other peaks that correspond to Mg, Li, or Mg-Li alloy, was shown by XRD. On the other hand, inductively coupled plasma tests showed the presence of both Mg and Li. Such composite deposits might work as anodes for rechargeable magnesium batteries.[15]

Recent research by Tran et al. has evaluated the performance of $Mg(TFSI)_2$/acetonitrile (AN) solution with stainless steel (SS) current collectors and Chevrel-phase Mo_6S_8 cathode material.[16] The high oxidation stability of acetonitrile makes it a highly attractive solvent. Stainless steel was tested mainly due to its common use in commercial cells. The SS electrode was operational between –0.2 V (AN reduction) and 2.8 V (SS corrosion), while no Mg deposition was observed. Although the oxidation stability window was quite low (2.8 V), it is still slightly higher than the oxidation window that is obtained with Grignard-based reagents (2.5 V). Reversible Mg intercalation/deintercalation from a $Mg(TFSI)_2$/AN into Chevrel-phase was demonstrated (Figure 4b).[16] However, since no Mg reversible deposition/stripping has been reported from $Mg(TFSI)_2$/AN solutions, it is most likely that decomposition of solution species occurs at the negative electrode during cycling.

The challenge of cathode materials: Intrinsic problems of slow Mg ion insertion

The functioning of cathodes in rechargeable Li or Mg batteries is based on the solid-state diffusion of Li^+ or Mg^{2+} ions (i.e., on their hopping between available sites in the crystal structure of intercalation compounds or hosts). The hopping is accompanied by charge transfer: The host atoms, commonly transition metals, have to accept the electrons associated with the ion insertion. In contrast to the Li^+ case, Mg ion diffusion in solids at room temperature (RT) is intrinsically slow due to the divalent character of Mg^{2+} cations (these cations have similar ionic radii of 0.76 Å for Li^+ and 0.72 Å for Mg^{2+} [17]). To illustrate this, **Figure 5** presents the voltage versus capacity curves obtained by Amatucci et al. for Li and Mg intercalation into nano-sized V_2O_5.[18] In the Li system, the curves achieved upon discharge and charge are very close to each other, indicating the fast kinetics of the electrochemical reaction between Li and V_2O_5. In contrast, in the Mg system, the process is slow: The potential of Mg de-insertion is 0.35 V higher than that of Mg insertion. (The current density was equal to 7.6 mA/g in both experiments.)

Thus far, the only materials that provide fast and reversible Mg insertion at RT are the Chevrel phases, $Mo_6S_{8-x}Se_x$ ($0 \le x \le 1$) and $CuMo_6S_8$.[5,19–21] The reason for this is the presence of Mo_6-clusters in their crystal structure (**Figure 6**a), which can easily adopt two Mg electrons.[22,23] The solid-state synthesis of Chevrel phases is relatively simple,[24,25] and even in the microcrystalline form, the material shows excellent cycleability (more than 3000 cycles in prototype Mg battery testing, see Figure 6b).[19] Due to a low working potential (1.1 V versus Mg^{2+}/Mg) and a limited capacity (120 mAh/g), Mg

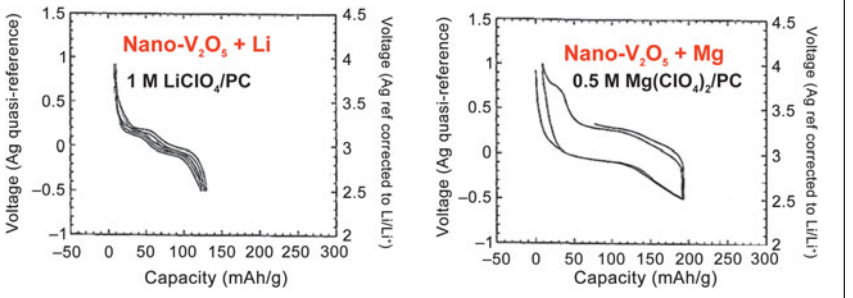


Figure 5. Slow ionic transport as a basic problem of Mg ion insertion cathodes: Comparison of Li- and Mg-ion intercalation into nano-sized V_2O_5 electrodes. The voltage is shown versus Ag (the left *y*-axis) and Li (the right *y*-axis) references. Mg^{2+} ion diffusion in common intercalation compounds is fundamentally slower than that for Li^+.[18] Note: PC, propylene carbonate.

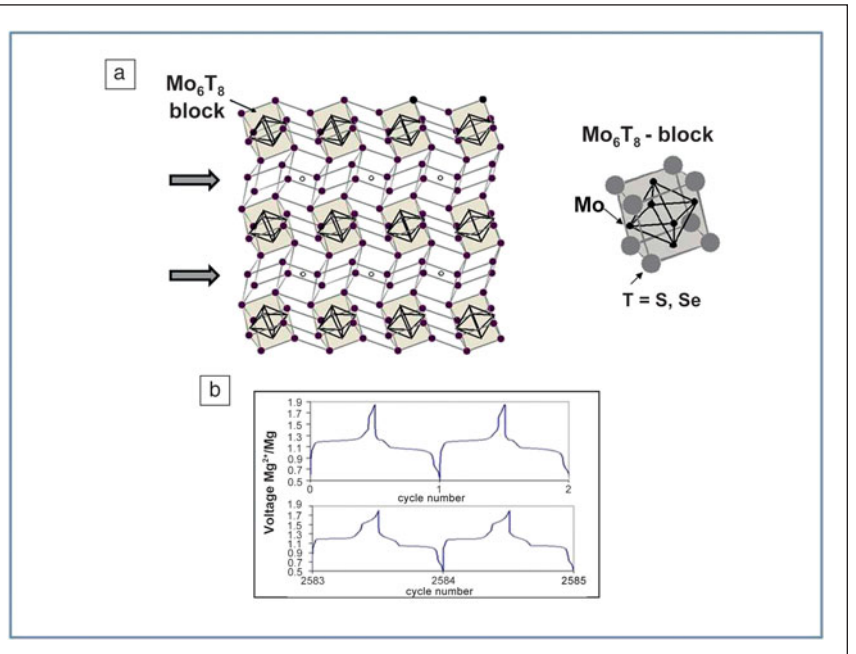


Figure 6. (a) The crystal structure of Chevrel phases. One of the directions of ionic transport in the channels between the Mo_6T_8 blocks is shown by arrows. The centers of the largest cavities available for cation insertion are marked by empty circles. The structure of the Mo_6T_8 clusters is presented separately on the right.[23] (b) Exceptionally stable electrochemical behavior of Chevrel phases: Typical voltage profiles of the first cycles and after prolonged cycling of Mg-$Mg_xMo_6S_8$ battery prototypes. Crystal structure of Chevrel phases composed of Mo_6 clusters ensures exceptionally fast and reversible Mg insertion at room temperature.[19]

https://doi.org/10.1557/mrs.2014.61 Published online by Cambridge University Press

batteries based on Chevrel phase cathodes are not really competitive with Li batteries, but the material serves as a standard cathode for checking the activity of new Mg electrolyte solutions.[26–28] The exceptional intercalation properties of Chevrel phases are also used in membranes for selective transfer of divalent cations between two electrolyte solutions.[29,30]

Recent studies of Mg cathodes have focused on classic hosts (see later in text), which have a high operating voltage and large capacity in Li batteries (normally, the voltage that can be obtained from a given host in Mg batteries is about 1 V lower than that in parallel Li batteries[31]). In their pioneering work, Gregory et al. showed a Mg intercalation ability for 15 different hosts, including oxides, sulfides, and borides.[3] This ability was confirmed in subsequent studies for V_2O_5,[18,32] hydrated vanadium bronzes,[33,34] orthorombic MoO_3,[35] cation-deficient spinel $Mn_{2.15}Co_{0.37}O_4$,[36] olivines $MgMnSiO_4$ and $MgCoSiO_4$,[37,38] sodium superionic conductors-type $Mg_{0.5}Ti_2(PO_4)_3$ and its derivatives,[39,40] different types of MnO_2,[41,42] and fluorinated graphite.[43,44]

In spite of the expected increase in the operating voltage, these studies revealed a key, persistent problem of slow Mg^{2+} ion motion in all the hosts, even in their nanometric form. For example, Ichitsubo et al. demonstrated that the Mg batteries based on disordered spinel $MgCo_2O_4$ or rock salt $Mg_{0.67}Ni_{1.33}O_2$ are sufficient to switch on a blue diode with a 2.6 V bandgap, but due to the slow Mg diffusion in these materials, only a partial charge of the batteries is possible, while the 4%-charge of $MgCo_2O_4$ and 50%-charge of $Mg_{0.67}Ni_{1.33}O_2$ take about 300 and 150 h, respectively.[45] Contrary to these results, first-principle calculations by Ling and Musino showed that Mg mobility in compounds such as post-spinel $MgMn_2O_4$ ($CaFe_2O_4$ structural type) should be comparable to that of Li,[46] but, as far as we know, this prediction has not yet been confirmed in practice.

Thus, the aim of the majority of recent studies has been to fundamentally improve Mg ion transport in classic hosts by modifying their morphology and even their layered atomic arrangement (e.g., by using TiS_2 nanotubes,[47] highly exfoliated MoS_2,[48] and V_2O_5-gel/carbon composites).[49,50] **Figure 7**a–b compares the common crystal structure of V_2O_5 with that of V_2O_5•nH_2O gel. As can be seen, square-pyramidal oxygen coordination around V in a common structure transforms into an octahedral one in the V_2O_5 gel.[51] Figure 7c illustrates the ribbon-like texture of the V_2O_5 aerogel.[52] Such structure and morphology modifications result in the change of the Mg intercalation mechanism: In addition to bulk insertion, typical for microcrystalline material, Mg^{2+} ions are absorbed on the surface of the active mass, and their transport is fast because it proceeds partially in the electrolyte solution. The larger the surface area available for Mg absorption, the higher is the material capacity. The main problem in such systems is obtaining stable electrochemical cycling by avoiding parasitic reactions between active material with large surface area and the electrolyte solution. A typical example of this problem is batteries based on TiS_2 nanotubes with a discharge capacity of 235 mAh/g (at current density of 10 mA/g) in the first cycle, which decreases down to 185 mAh/g after 80 cycles or after battery heating to 60°C,[47] (a typical elevated temperature for checking the thermal stability of battery systems during cycling).

Nevertheless, Liang et al. demonstrated a relatively high operating voltage of 1.8 V and a stable discharge capacity of 170 mAh/g (at a discharge rate of 20 mA/g) during 50 cycles for highly exfoliated graphene-like MoS_2 (**Figure 8**a).[48] Essentially higher capacity (300 mAh/g at a current density of

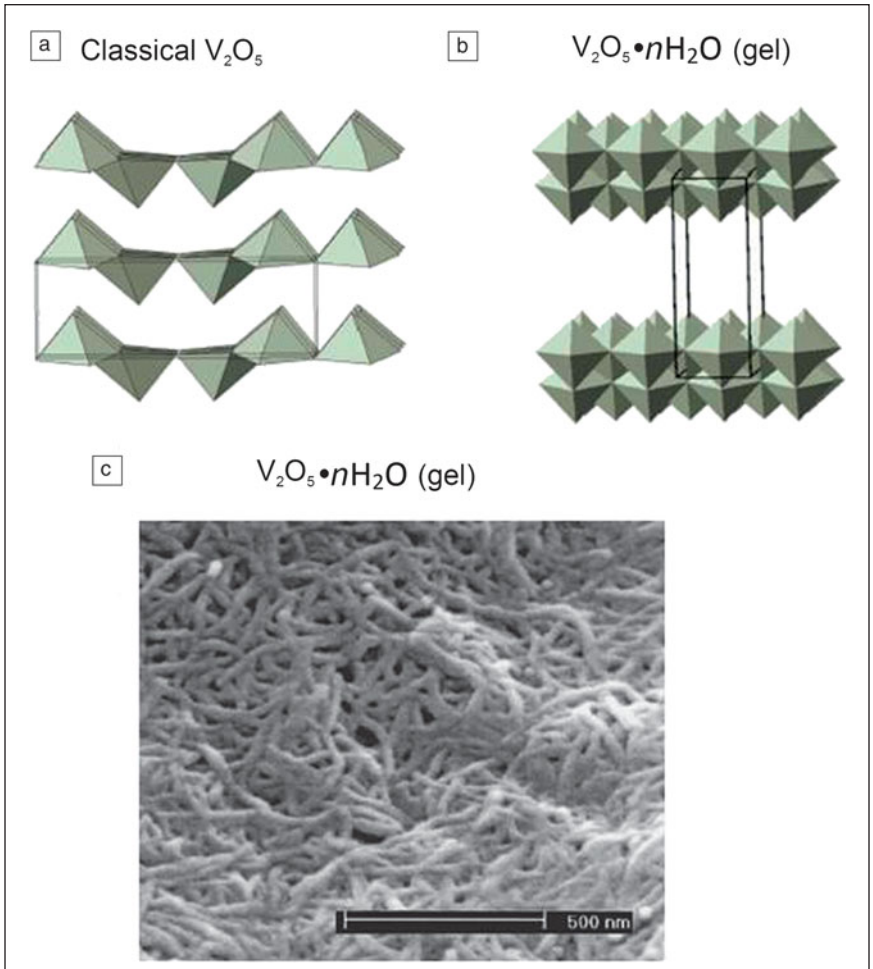


Figure 7. Crystal structure of (a) normal V_2O_5 and (b) V_2O_5 • nH_2O xerogel.[51] (c) Scanning electron microscope micrograph of dried V_2O_5 aerogel particles (both the V_2O_5 xerogel and V_2O_5 aerogel insert Mg ions).[52] The morphology and the crystal structure of common intercalation compounds should be modified to ensure fast and reversible transport of divalent Mg cations.

https://doi.org/10.1557/mrs.2014.61 Published online by Cambridge University Press

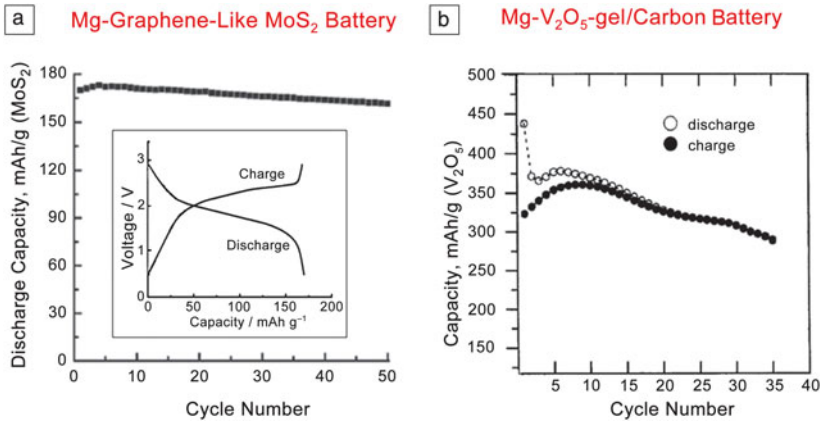


Figure 8. (a) Cycleability of highly exfoliated graphene-like MoS_2 versus Mg in $Mg(AlCl_3Bu)_2$/tetrahydrofuran (dichloro complex solution, current density of 20 mA/g). The insert shows a typical voltage profile of the cell.[48] (b) Cycleability of V_2O_5 (aerogel)/carbon composite electrodes versus Mg in 1 M $Mg(ClO_4)_2$/acetonitrile (current density of 17 mA/g).[50] Promising electrochemical behavior was obtained for graphene-like MoS_2 and V_2O_5-gel/carbon composite cathodes. Note: Bu, butyl.

0.17 mA/g) was obtained for the V_2O_5-gel/carbon composites (Figure 8b).[49,50] Interestingly, for both systems, the potential of Mg ion intercalation is close to or even higher than the insertion potential of Li ions. For example, the graphene-like MoS_2/carbon composite was recommended as an anode for Li-ion batteries because its reduction occurs at potentials lower than 1.8 V versus Li^+/Li.[53] These close values in potentials of Li and Mg insertions are in contradiction with the expected 1 V difference, which is typical for the normal bulk insertion (see previous text). This unusual phenomenon can be explained by solvent co-intercalation (insertion of solvated Mg^{2+} ions) into the host crystal structure.[31] In the case of co-intercalation, the average working voltage of the battery increases due to the energy gain between full Mg^{2+} ion solvation on the anode side and only partial desolvation on the cathode side. Solvent co-intercalation should also improve the kinetics of Mg ions insertion by effective screening of the high Mg^{2+} ions charge, but it may have a negative influence on the material capacity.[31]

As can be seen, the development of cathode materials convenient for rechargeable Mg batteries remains an ongoing challenge due to strict requirements for the intercalation compound that ensures fast Mg^{2+} ion transport in combination with a high operating voltage.

Conclusions

The realization of secondary magnesium batteries requires the development of two elements: (1) electrolyte solutions containing mobile Mg ions in which Mg electrodes are bare, passivation film free, and thus enable reversible Mg deposition; and (2) intercalation compounds that allow fast diffusion of Mg^{+2} ions into them and exhibit high specific capacity, operating potentials, and reversibility.

The discovery that $Mg(TFSI)_2$ (TFSI = trifluoromethanesulfonimide)–ethers-based solutions support reversible magnesium deposition might pave the way for the development of a new family of resilient, practically feasible, electrolyte solutions for rechargeable Mg batteries with high capacity/high voltage cathodes.

As cathode materials, only two families of materials show intercalation by Mg ions with sufficiently fast kinetics, capacity, and reversibility. Unfortunately, both exhibit significant shortcomings. Understanding what influences the solid-state diffusion mechanism of the doubly charged Mg ions might yield a clue as to how to tackle this complicated problem. Alternatively, redox cathodes that do not rely on solid-state diffusion may prove to be a better direction.

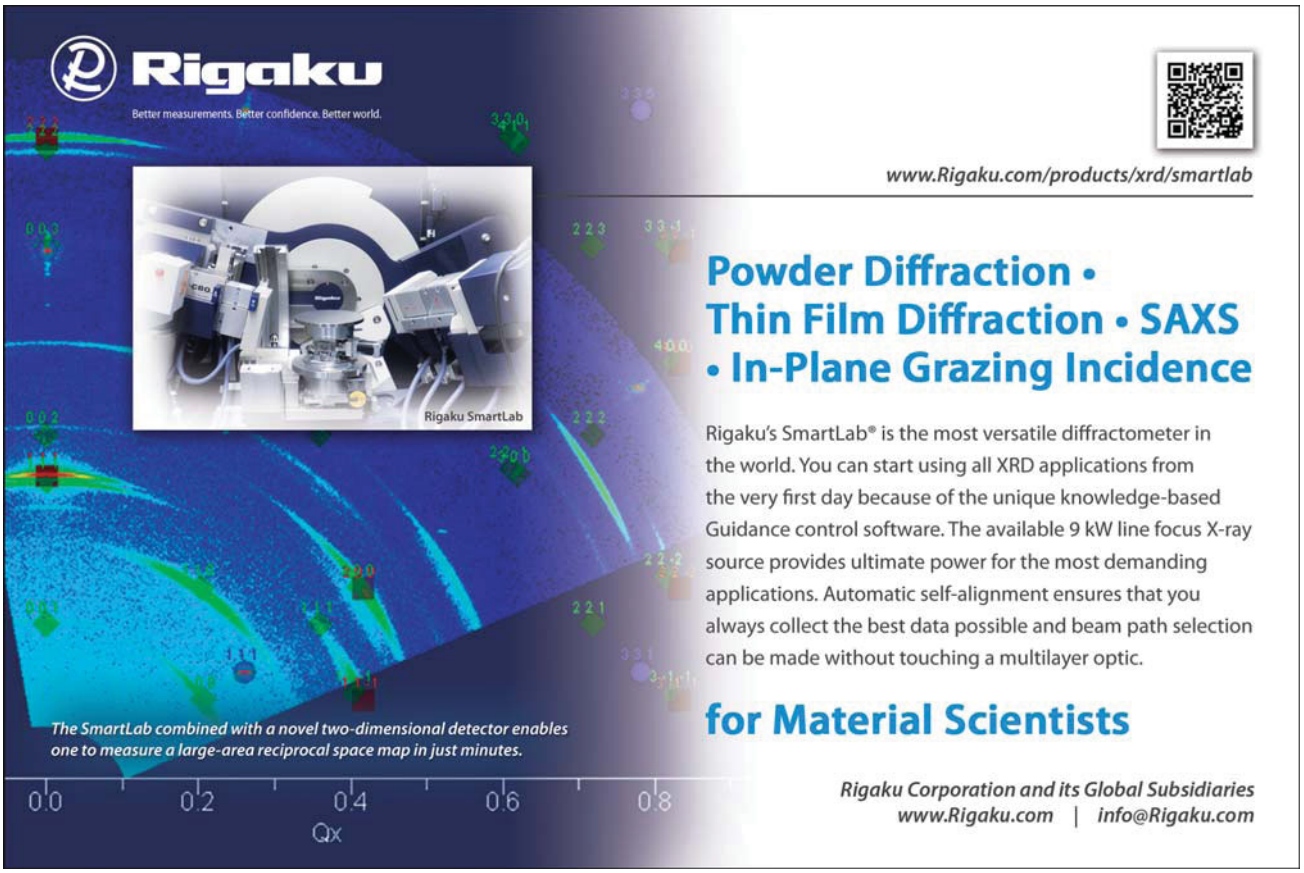
Despite several breakthroughs in the field of non-aqueous Mg electrochemistry described in this article, much is left to be desired for both the anode-electrolyte solution and the cathode. However, since Mg is so abundant, nontoxic, and non-hazardous and possesses many other advantages over Li and other possible anode materials, it makes sense to invest efforts into the realization of this technology. The prototypes of rechargeable Mg batteries presented so far demonstrate a battery technology that may be able to rival the commonly used lead-acid and Ni-Cd batteries in terms of energy density and highly prolonged cycle life in a wide temperature domain. While Mg batteries are not supposed to outperform Li-ion batteries in terms of energy density and rates, they may have advantages in terms of prolonged cycle life, safety, and abundance of materials. Further development of new electrolyte solutions for reversible Mg deposition operating in wide electrochemical windows described herein and high capacity reversible Mg insertion cathode materials (still under development but with promising results thus far) will enable useful and practically attractive rechargeable Mg batteries for a wide spectrum of load leveling applications.

References

1. Y. Gofer, O. Chusid, D. Aurbach, in *Encyclopedia of Electrochemical Power Sources*, J. Garche, Ed. (Elsevier, Amsterdam, 2009), pp. 285–301.
2. L.W. Gaddum, H.E. French, *J. Am. Chem. Soc.* **49**, 1295 (1927).
3. T.D. Gregory, R.J. Hoffman, R.C. Winterton, *J. Electrochem. Soc.* **137**, 775 (1990).
4. R. Chevrel, M. Sergent, J. Prigent, *J. Solid State Chem.* **3**, 515 (1971).
5. D. Aurbach, Z. Lu, A. Schechter, Y. Gofer, H. Gizbar, R. Turgeman, Y. Cohen, M. Moshkovich, E. Levi, *Nature* **407**, 724 (2000).
6. Y. Gofer, R. Turgeman, H. Cohen, D. Aurbach, *Langmuir* **19**, 2344 (2003).
7. N. Amir, Y. Vestfrid, O. Chusid, Y. Gofer, D. Aurbach, *J. Power Sources* **174**, 1234 (2007).
8. D. Aurbach, H. Gizbar, A. Schechter, O. Chusid, H.E. Gottlieb, Y. Gofer, I. Goldberg, *J. Electrochem. Soc.* **149**, A115 (2002).
9. O. Chusid, Y. Gofer, H. Gizbar, Y. Vestfrid, E. Levi, D. Aurbach, I. Riech, *Adv. Mater.* **15**, 627 (2003).
10. Y. Vestfried, O. Chusid, Y. Goffer, P. Aped, D. Aurbach, *Organometallics* **26**, 3130 (2007).
11. N. Pour, Y. Gofer, D.T. Major, D. Aurbach, *J. Am. Chem. Soc.* **133**, 6270 (2011).
12. C. Liebenow, Z. Yang, P. Lobitz, *Electrochem. Commun.* **2**, 641 (2000).

https://doi.org/10.1557/mrs.2014.61 Published online by Cambridge University Press

13. H.S. Kim, T.S. Arthur, G.D. Allred, J. Zajicek, J.G. Newman, A.E. Rodnyansky, A.G. Oliver, W.C. Boggess, J. Muldoon, *Nat. Commun.* **2**, 427 (2011).
14. R.E. Doe, R. Han, J. Hwang, A.J. Gmitter, I. Shterenberg, H.D. Yoo, N. Pour, D. Aurbach, *Chem. Commun.* **50**, 243 (2014).
15. O. Shimamura, N. Yoshimoto, M. Matsumoto, M. Egashia, M. Morita, *J. Power Sources* **196**, 1586 (2011).
16. T.T. Tran, W.M. Lamanna, M.N. Obrovac, *J. Electrochem. Soc.* **159**, A2005 (2012).
17. R. Shannon, *Acta Crystallogr. Sect. A: Found. Crystallogr.* **32**, 751 (1976).
18. G.G. Amatucci, F. Badway, A. Singhal, B. Beaudoin, G. Skandan, T. Bowmer, I. Plitza, N. Pereira, T. Chapman, R. Jaworski, *J. Electrochem. Soc.* **148**, A940 (2001).
19. D. Aurbach, I. Weissman, Y. Gofer, E. Levi, *Chem. Rec.* **3**, 61 (2003).
20. D. Aurbach, G.S. Suresh, E. Levi, A. Mitelman, O. Mizrahi, O. Chusid, M. Brunelli, *Adv. Mater.* **19**, 4260 (2007).
21. A. Mitelman, M.D. Levi, E. Lancry, E. Levi, D. Aurbach, *Chem. Commun.* **44**, 4212 (2007).
22. E. Levi, M.D. Levi, O. Chasid, D. Aurbach, *J. Electroceram.* **22**, 13 (2009).
23. E. Levi, G. Gershinsky, D. Aurbach, O. Isnard, G. Ceder, *Chem. Mater.* **21**, 1390 (2009).
24. E. Lancry, E. Levi, A. Mitelman, S. Malovany, D. Aurbach, *J. Solid State Chem.* **179**, 1879 (2006).
25. G. Gershinsky, O. Haik, G. Salitra, J. Grinblat, E. Levi, G.D. Nessim, E. Zinigrad, D. Aurbach, *J. Solid State Chem.* **188**, 50 (2012).
26. R. Mohtadi, M. Matsui, T.S. Arthur, S.-J. Hwang, *Angew. Chem. Int. Ed.* **51** (39), 9780 (2012).
27. Y. Shao, T. Liu, G. Li, M. Gu, Z. Nie, M. Engelhard, J. Xiao, D. Lv, C. Wang, J.G. Zhang, J. Liu, *Sci. Rep.* **3**, 3130 (2013).
28. J. Zhu, Y. Guo, J. Yang, Y. Nuli, F. Zhang, J. Wang, S.-I. Hirano, *J. Power Sources* **248**, 690 (2014).
29. S. Seghir, C. Boulanger, S. Diliberto, M. Potel, J.M. Lecuire, *Electrochim. Acta* **55**, 1097 (2010).
30. E. Guyot, S. Seghir, J.M. Lecuire, C. Boulanger, M.D. Levi, Y. Shilina, V. Dargel, D. Aurbach, *J. Electrochem. Soc.* **160**, A420 (2013).
31. E. Levi, Y. Gofer, D. Aurbach, *Chem. Mater.* **22**, 860 (2010).
32. P. Novak, J. Desilvestro, *J. Electrochem. Soc.* **140**, 140 (1993).
33. P. Novák, W. Scheifele, F. Joho, O. Haas, *J. Electrochem. Soc.* **142**, 2544 (1995).
34. P. Novák, W. Scheifele, O. Haas, *J. Power Sources* **54**, 479 (1995).
35. M.E. Spahr, P. Novak, O. Haas, R. Nesper, *J. Power Sources* **54**, 346 (1995).
36. L. Sanchez, J.-P. Pereira-Ramos, *J. Mater. Chem.* **7**, 471 (1997).
37. Z. Feng, J. Yang, Y. NuLi, J. Wang, *J. Power Sources* **184**, 604 (2008).
38. Y. Zheng, Y. NuLi, Q. Chen, Y. Wang, J. Yang, J. Wang, *Electrochim. Acta* **66**, 75 (2012).
39. K. Makino, Y. Katayama, T. Miura, T. Kishi, *J. Power Sources* **99**, 66 (2001).
40. K. Makino, Y. Katayama, T. Miura, T. Kishi, *J. Power Sources* **112**, 85 (2002).
41. R. Zhang, X. Yu, K.-W. Nam, C. Ling, T.S. Arthur, W. Song, A.M. Knapp, S.N. Ehrlich, X.-Q. Yang, M. Matsui, *Electrochem. Commun.* **23**, 110 (2012).
42. S. Rasul, S. Suzuki, S. Yamaguchi, M. Miyayama, *Electrochim. Acta* **82**, 243 (2012).
43. J. Giraudet, D. Claves, K. Guerin, M. Dubois, A. Houdayer, F. Masin, A. Hamwi, *J. Power Sources* **173**, 592 (2007).
44. J.V. Rani, S.B. Rushi, V. Kanakaiah, S. Palaniappan, *J. Electrochem. Soc.* **158**, A1031 (2011).
45. T. Ichitsubo, T. Adachi, S. Yagi, T. Doi, *J. Mater. Chem.* **21**, 11764 (2011).
46. C. Ling, F. Mizuno, *Chem. Mater.* **25**, 3062 (2013).
47. Z.L. Tao, L.N. Xu, X.L. Gou, J. Chen, H.T. Yuan, *Chem. Commun.* 2080 (2004).
48. Y. Liang, R. Feng, S. Yang, H. Ma, J. Liang, J. Chen, *Adv. Mater.* **23**, 640 (2011).
49. D. Imamura, M. Miyayama, *Solid State Ionics* **161**, 173 (2003).
50. D. Imamura, M. Miyayama, M. Hibino, T. Kudo, *J. Electrochem. Soc.* **150**, A753 (2003).
51. V. Petkov, P.Y. Zavalij, S. Lutta, M.S. Whittingham, V. Parvanov, S. Shastri, *Phys. Rev. B* **69**, 085410 (2004).
52. G. Sudant, E. Baudrin, B. Dunn, J.-M. Tarascon, *J. Electrochem. Soc.* **151**, A666 (2004).
53. K. Chang, W. Chen, L. Ma, H. Li, H. Li, F. Huang, Z. Xu, Q. Zhang, J.-Y. Lee, *J. Mater. Chem.* **21**, 6251 (2011). □



https://doi.org/10.1557/mrs.2014.61 Published online by Cambridge University Press